The International Workshop on Low-X Physics
Rehovot+Eilat (Israel), May 30th-June4th 2013

Combined Inclusive Diffractive Cross Sections Measured with Forward Proton Spectrometers at HERA

Marta Ruspa
Univ. Piemonte Orientale & INFN-Torino, Italy

Diffractive DIS at HERA

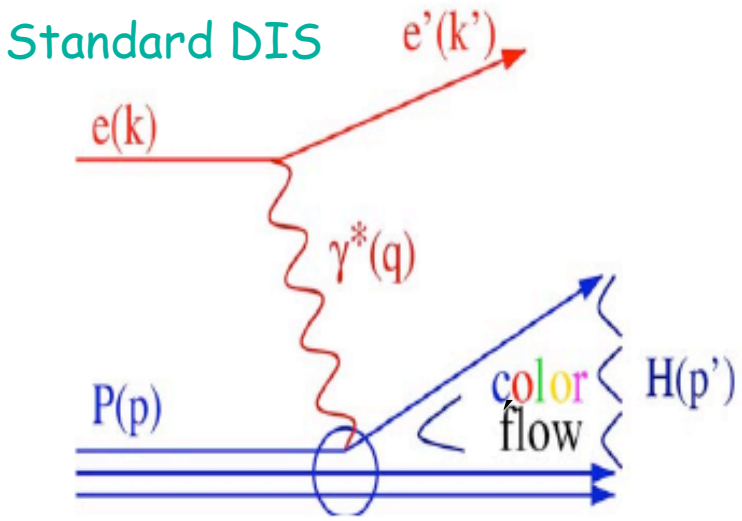

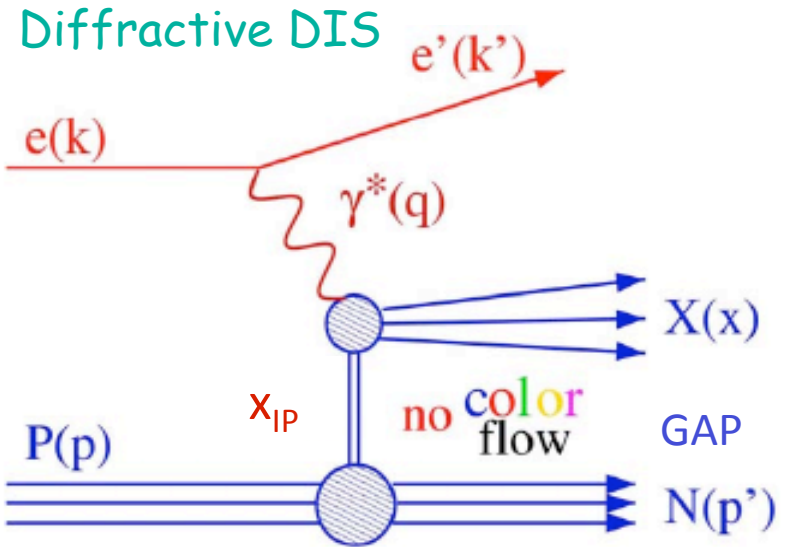

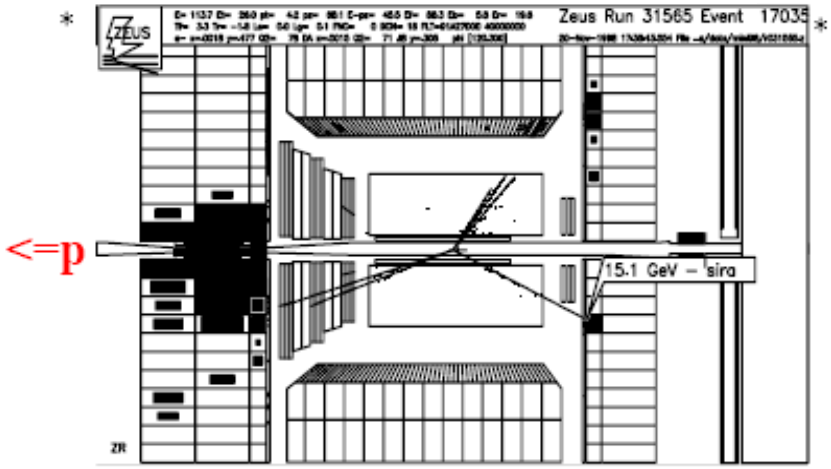

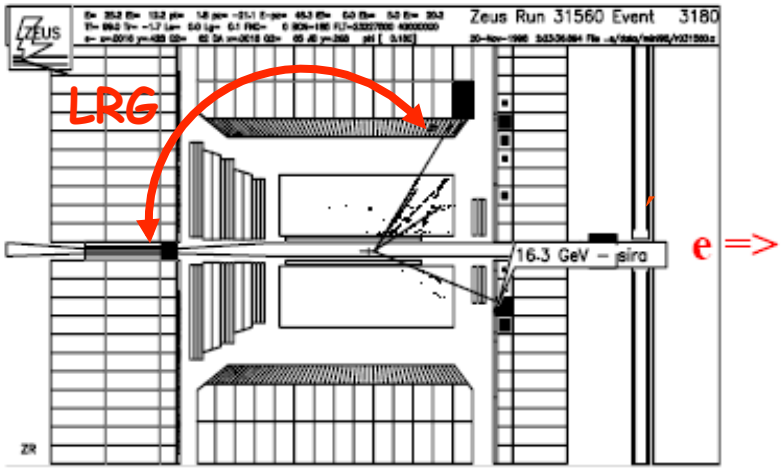

Kinematics of diffractive DIS

Q^2 = virtuality of photon =
= (4-momentum exchanged at e vertex)^2

W = invariant mass of γ^*-p system

M_X = invariant mass of γ^* -IP system

x_{IP} = fraction of proton's momentum carried by IP

β = Bjorken's variable for the IP
= fraction of IP momentum carried by struck quark
= x/x_{IP}

t = (4-momentum exchanged at p vertex)^2
typically: $|t|<1$ GeV^2

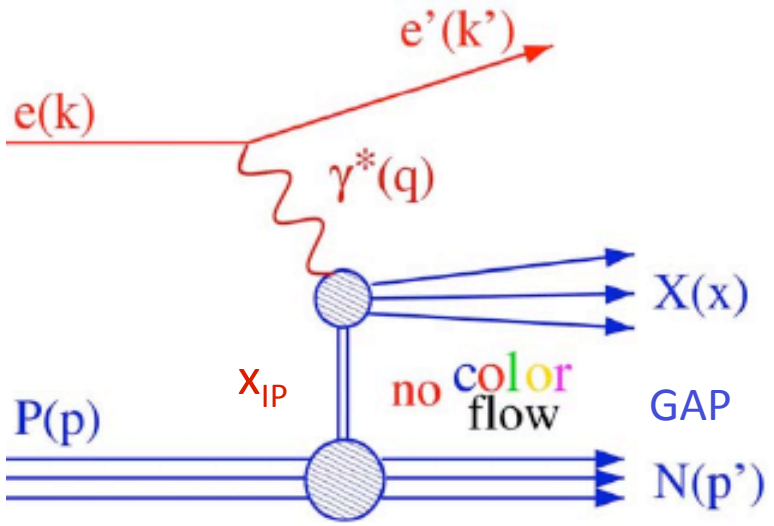

- Single diffraction: N=proton
- Double diffraction: proton-dissociative system N

→ represents a relevant background

Diffractive cross section & structure functions

- Diffractive cross section

$$\frac{d\sigma^{D}_{\gamma^* p}}{dM_X} = \frac{\pi Q^2 W}{\alpha(1+(1-y)^2)} \cdot \frac{d^3\sigma^{D}_{ep\to e'Xp'}}{dQ^2 dM_X dW}$$

$$\frac{d\sigma}{dt} \sim e^{bt}$$

- Diffractive structure function $F_2^{D(4)}$ and reduced cross sections $\sigma_r^{D(4)}$ and $\sigma_r^{D(3)}$

$$\frac{d^2\sigma^{ep\to e'Xp'}}{d\beta dQ^2 dx_{IP} dt} = \frac{4\pi\alpha^2}{\beta Q^4}\left[1 - y + \frac{y^2}{2(1+R^D)}\right] \cdot F_2^{D(4)}(\beta, Q^2, x_{IP}, t)$$

$$= \frac{4\pi\alpha^2}{\beta Q^4}\left[1 - y + \frac{y^2}{2}\right] \cdot \sigma_r^{D(4)}(\beta, Q^2, x_{IP}, t)$$

$$\sigma_r^{D(3)}(\beta, Q^2, x_{IP}) = \int \sigma_r^{D(4)}(\beta, Q^2, x_{IP}, t)\, dt$$

- $R^D = \sigma_L^{\gamma^* p\to Xp} / \sigma_T^{\gamma^* p\to Xp}$; $\sigma_r^D = F_2^D$ when $R^D = 0$

Diffractive cross section & structure functions

- Diffractive cross section

$$\frac{d\sigma^{D}_{\gamma^* p}}{dM_X} = \frac{\pi Q^2 W}{\alpha(1+(1-y)^2)} \cdot \frac{d^3\sigma^{D}_{ep\to e'Xp'}}{dQ^2 dM_X dW}$$

$$\frac{d\sigma}{dt} \sim e^{bt}$$

- Diffractive structure function $F_2^{D(4)}$ and reduced cross sections $\sigma_r^{D(4)}$ and $\sigma_r^{D(3)}$

$$\frac{d^2\sigma^{ep\to e'Xp'}}{d\beta dQ^2 dx_{IP} dt} = \frac{4\pi\alpha^2}{\beta Q^4}\left[1 - y + \frac{y^2}{2(1+R^D)}\right] \cdot F_2^{D(4)}(\beta, Q^2, x_{IP}, t)$$

$$= \frac{4\pi\alpha^2}{\beta Q^4}\left[1 - y + \frac{y^2}{2}\right] \cdot \sigma_r^{D(4)}(\beta, Q^2, x_{IP}, t)$$

$$\sigma_r^{D(3)}(\beta, Q^2, x_{IP}) = \int \sigma_r^{D(4)}(\beta, Q^2, x_{IP}, t)\, dt$$

- $R^D = \sigma_L^{\gamma^* p\to Xp} / \sigma_T^{\gamma^* p\to Xp}$; $\sigma_r^D = F_2^D$ when $R^D = 0$

Diffractive cross section & structure functions

- Diffractive cross section

$$\frac{d\sigma^{D}_{\gamma^* p}}{dM_X} = \frac{\pi Q^2 W}{\alpha(1+(1-y)^2)} \cdot \frac{d^3\sigma^{D}_{ep\to e'Xp'}}{dQ^2 dM_X dW}$$

$$\frac{d\sigma}{dt} \sim e^{bt}$$

- Diffractive structure function $F_2^{D(4)}$ and reduced cross sections $\sigma_r^{D(4)}$ and $\sigma_r^{D(3)}$

$$\frac{d^2\sigma^{ep\to e'Xp'}}{d\beta dQ^2 dx_{IP} dt} = \frac{4\pi\alpha^2}{\beta Q^4}\left[1 - y + \frac{y^2}{2(1+R^D)}\right] \cdot F_2^{D(4)}(\beta, Q^2, x_{IP}, t)$$

$$= \frac{4\pi\alpha^2}{\beta Q^4}\left[1 - y + \frac{y^2}{2}\right] \cdot \sigma_r^{D(4)}(\beta, Q^2, x_{IP}, t)$$

$$\sigma_r^{D(3)}(\beta, Q^2, x_{IP}) = \int \sigma_r^{D(4)}(\beta, Q^2, x_{IP}, t)\, dt$$

- $R^D = \sigma_L^{\gamma^* p\to Xp} / \sigma_T^{\gamma^* p\to Xp}$; $\sigma_r^D = F_2^D$ when $R^D = 0$

Diffractive cross section & structure functions

- Diffractive cross section

$$\frac{d\sigma^{D}_{\gamma^* p}}{dM_X} = \frac{\pi Q^2 W}{\alpha(1+(1-y)^2)} \cdot \frac{d^3\sigma^{D}_{ep\to e'Xp'}}{dQ^2 dM_X dW}$$

$$\frac{d\sigma}{dt} \sim e^{bt}$$

- Diffractive structure function $F_2^{D(4)}$ and reduced cross sections $\sigma_r^{D(4)}$ and $\sigma_r^{D(3)}$

$$\frac{d^2\sigma^{ep\to e'Xp'}}{d\beta dQ^2 dx_{IP} dt} = \frac{4\pi\alpha^2}{\beta Q^4}\left[1 - y + \frac{y^2}{2(1+R^D)}\right] \cdot F_2^{D(4)}(\beta, Q^2, x_{IP}, t)$$

$$= \frac{4\pi\alpha^2}{\beta Q^4}\left[1 - y + \frac{y^2}{2}\right] \cdot \sigma_r^{D(4)}(\beta, Q^2, x_{IP}, t)$$

$$\sigma_r^{D(3)}(\beta, Q^2, x_{IP}) = \int \sigma_r^{D(4)}(\beta, Q^2, x_{IP}, t)\, dt$$

- $R^D = \sigma_L^{\gamma^* p\to Xp} / \sigma_T^{\gamma^* p\to Xp}$; $\sigma_r^D = F_2^D$ when $R^D = 0$

Available publications

H1 LRG	H1 Collab., Eur. Phys. J. C48 (2006) 715 H1 Collab., Eur. Phys. J. C72 (2012) 2074
ZEUS LRG	ZEUS Collab., Nucl. Phys. B816 (2009) 1
H1 FPS	H1 Collab., Eur. Phys. J. C71 (2011) 1578 H1 Collab., Eur. Phys. J. C48 (2006) 749
ZEUS LPS	ZEUS Collab., Nucl. Phys. B816 (2009) 1 ZEUS Collab., Eur. Phys. J. C38 (2004) 43

Signatures and selection methods

Proton Spectrometer (PS) method

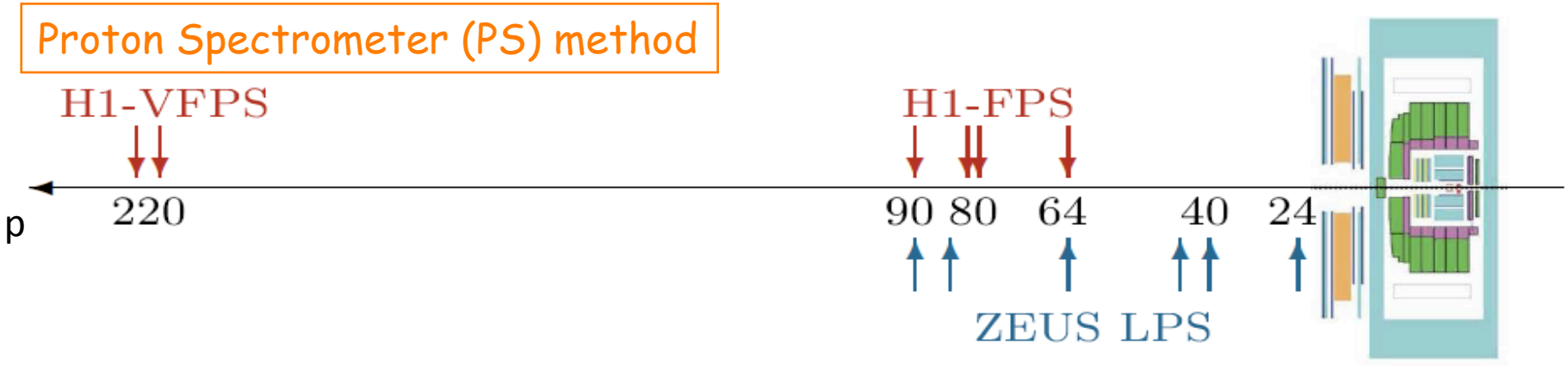

Large Rapidity Gap (LRG) method

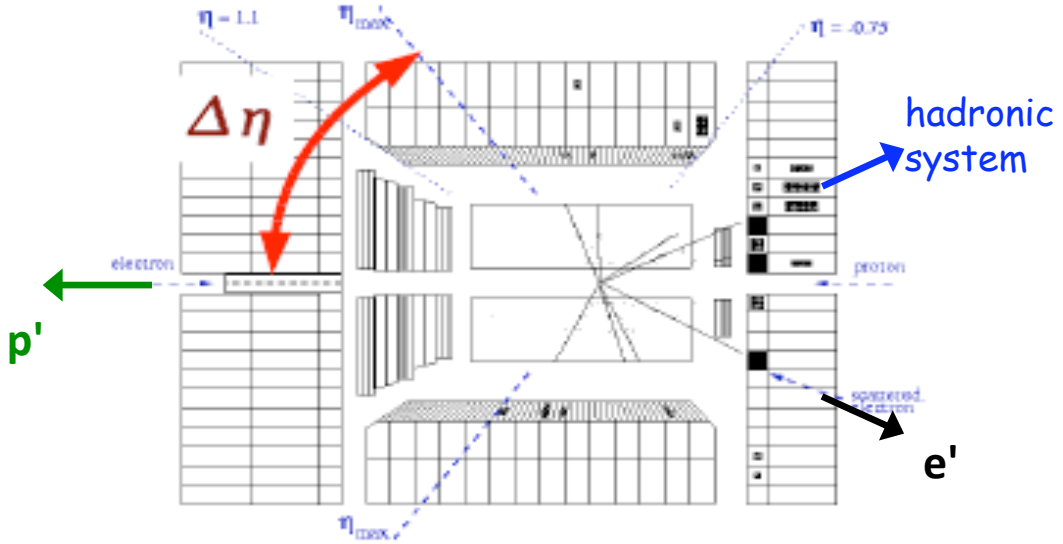

Signatures and selection methods

Proton Spectrometer (PS) method

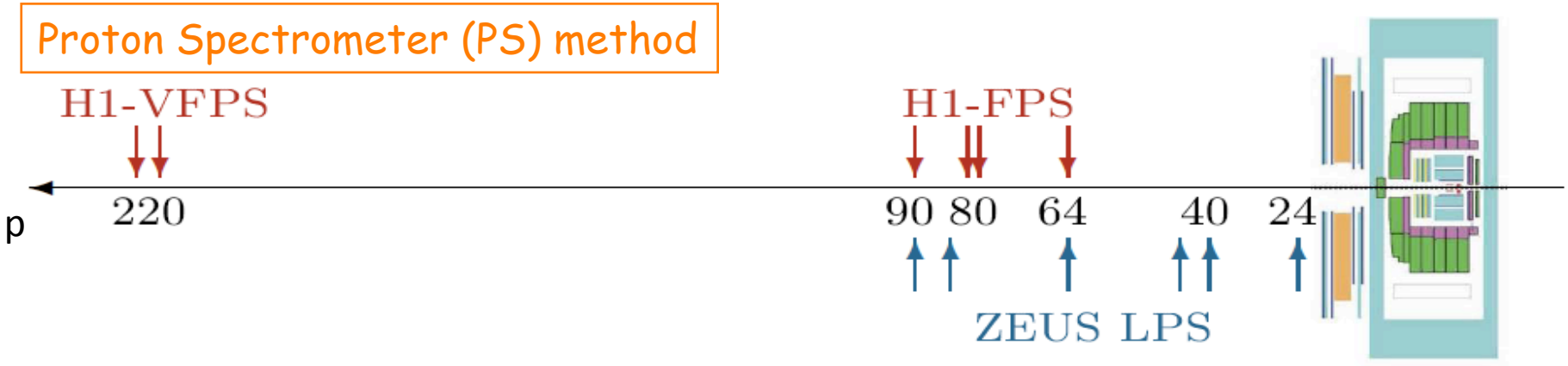

Large Rapidity Gap (LRG) method

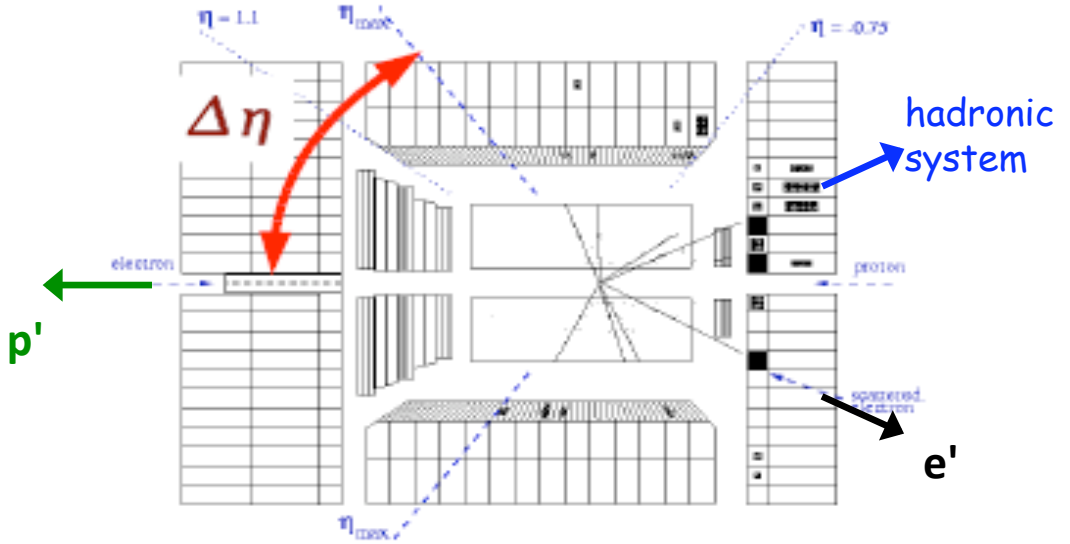

near perfect acceptance at low x_{IP}

p-diss contribution
no t measurement

Signatures and selection methods

Proton Spectrometer (PS) method

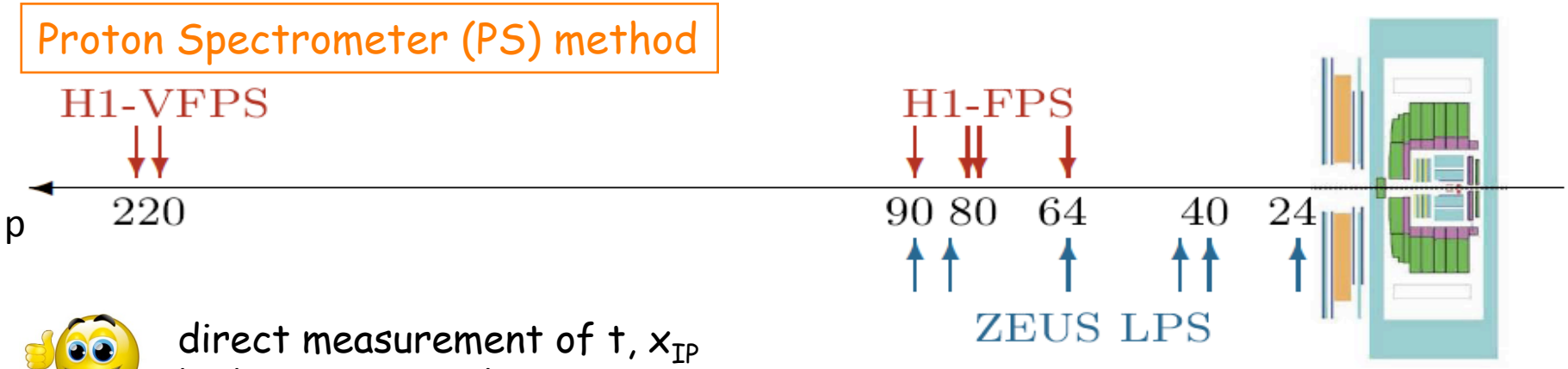

direct measurement of t, x_{IP}
high x_{IP} accessible
no p-diss contribution

low statistics

Large Rapidity Gap (LRG) method

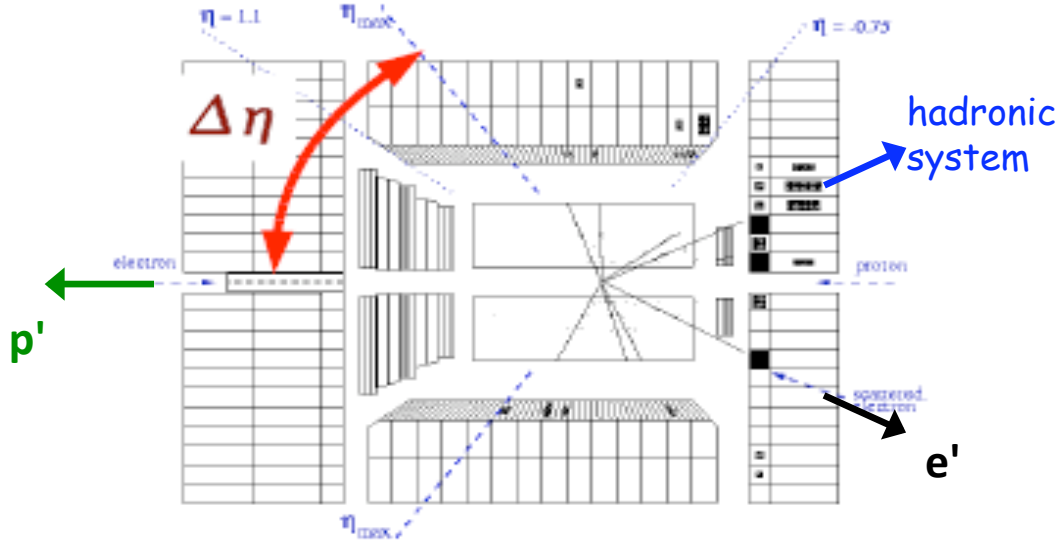

near perfect acceptance
at low x_{IP}

p-diss contribution
no t measurement

Available publications

H1 LRG	H1 Collab., Eur. Phys. J. C48 (2006) 715 H1 Collab., Eur. Phys. J. C72 (2012) 2074
ZEUS LRG	ZEUS Collab., Nucl. Phys. B816 (2009) 1
H1 FPS	H1 Collab., Eur. Phys. J. C71 (2011) 1578 H1 Collab., Eur. Phys. J. C48 (2006) 749
ZEUS LPS	ZEUS Collab., Nucl. Phys. B816 (2009) 1 ZEUS Collab., Eur. Phys. J. C38 (2004) 43

Consistent results from the two methods

Comparison H1-ZEUS

Combining the measurements can provide more precise and kinematically extended data than the individual sets

Available publications

H1 LRG	H1 Collab., Eur. Phys. J. C48 (2006) 715 H1 Collab., Eur. Phys. J. C72 (2012) 2074
ZEUS LRG	ZEUS Collab., Nucl. Phys. B816 (2009) 1
H1 FPS	H1 Collab., Eur. Phys. J. C71 (2011) 1578 H1 Collab., Eur. Phys. J. C48 (2006) 749
ZEUS LPS	ZEUS Collab., Nucl. Phys. B816 (2009) 1 ZEUS Collab., Eur. Phys. J. C38 (2004) 43

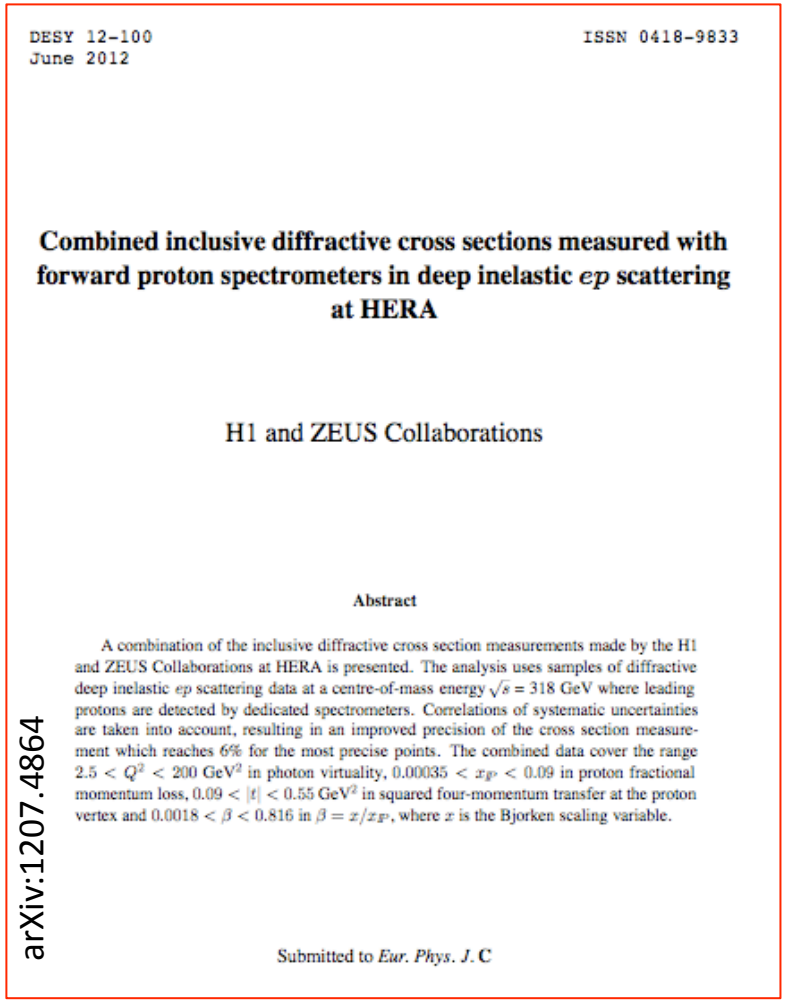

DESY 12-100
June 2012

ISSN 0418-9833

Combined inclusive diffractive cross sections measured with forward proton spectrometers in deep inelastic ep scattering at HERA

H1 and ZEUS Collaborations

Abstract

A combination of the inclusive diffractive cross section measurements made by the H1 and ZEUS Collaborations at HERA is presented. The analysis uses samples of diffractive deep inelastic ep scattering data at a centre-of-mass energy $\sqrt{s} = 318$ GeV where leading protons are detected by dedicated spectrometers. Correlations of systematic uncertainties are taken into account, resulting in an improved precision of the cross section measurement which reaches 6% for the most precise points. The combined data cover the range $2.5 < Q^2 < 200$ GeV^2 in photon virtuality, $0.00035 < x_{I\!P} < 0.09$ in proton fractional momentum loss, $0.09 < |t| < 0.55$ GeV^2 in squared four-momentum transfer at the proton vertex and $0.0018 < \beta < 0.816$ in $\beta = x/x_{I\!P}$, where x is the Bjorken scaling variable.

Submitted to *Eur. Phys. J.* C

Combining the measurements can provide more precise and kinematically extended data than the individual sets

Proton spectrometer results now combined
(first combination in diffraction at HERA!)

Data sets for combination

- H1 FPS HERA II
  [Eur.Phys.J. C71 (2011) 1578]
  Luminosity = 156.6 pb^{-1}
  Visible range $|t|$ = 0.1 – 0.7 GeV^2
  Norm unc ~ ± 6%

- H1 FPS HERA I
  [Eur.Phys.J. C48 (2006) 749]
  Luminosity = 28.4 pb^{-1}
  Visible range $|t|$ = 0.08 – 0.5 GeV^2
  Norm unc ~ ± 10%

- ZEUS LPS 2
  [Nucl.Phys. B816 (2009) 1]
  Luminosity = 32.6 pb^{-1}
  Visible range $|t|$ = 0.09 – 0.55 GeV^2
  Norm unc ~ +11 -7%

- ZEUS LPS 1
  [Eur.Phys.J. C38 (2004) 43]
  Luminosity = 3.6 pb^{-1}
  Visible range $|t|$ = 0.075 – 0.35 GeV^2
  Norm unc ~ +12% - 10%

$\sigma_r^{D(3)}$ combined

Data sets for combination

- H1 FPS HERA II
  [Eur.Phys.J. C71 (2011) 1578]
  Luminosity = 156.6 pb^{-1}
  Visible range $|t|$ = 0.1 – 0.7 GeV^2
  Norm unc ~ ± 6%

- H1 FPS HERA I
  [Eur.Phys.J. C48 (2006) 749]
  Luminosity = 28.4 pb^{-1}
  Visible range $|t|$ = 0.08 – 0.5 GeV^2
  Norm unc ~ ± 10%

- ZEUS LPS 2
  [Nucl.Phys. B816 (2009) 1]
  Luminosity = 32.6 pb^{-1}
  Visible range $|t|$ = 0.09 – 0.55 GeV^2
  Norm unc ~ +11 -7%

- ZEUS LPS 1
  [Eur.Phys.J. C38 (2004) 43]
  Luminosity = 3.6 pb^{-1}
  Visible range $|t|$ = 0.075 – 0.35 GeV^2
  Norm unc ~ +12% - 10%

$\sigma_r^{D(3)}$ combined

Main H1 and ZEUS detectors used to reconstruct Q^2, W and x, whereas M_x, ß, x_{IP} and t derived from FPS/LPS or from combined info H1+FPS/ZEUS+LPS

Data sets for combination

- H1 FPS HERA II
  [Eur.Phys.J. C71 (2011) 1578]
  Luminosity = 156.6 pb^{-1}
  Visible range $|t|$ = 0.1 – 0.7 GeV^2
  Norm unc ~ ± 6%

- H1 FPS HERA I
  [Eur.Phys.J. C48 (2006) 749]
  Luminosity = 28.4 pb^{-1}
  Visible range $|t|$ = 0.08 – 0.5 GeV^2
  Norm unc ~ ± 10%

- ZEUS LPS 2
  [Nucl.Phys. B816 (2009) 1]
  Luminosity = 32.6 pb^{-1}
  Visible range $|t|$ = 0.09 – 0.55 GeV^2
  Norm unc ~ +11 -7%

- ZEUS LPS 1
  [Eur.Phys.J. C38 (2004) 43]
  Luminosity = 3.6 pb^{-1}
  Visible range $|t|$ = 0.075 – 0.35 GeV^2
  Norm unc ~ +12% - 10%

$\sigma_r^{D(3)}$ combined

Main H1 and ZEUS detectors used to reconstruct Q^2, W and x, whereas M_x, ß, x_{IP} and t derived from FPS/LPS or from combined info H1+FPS/ZEUS+LPS

Combination performed in the ZEUS visible t range $|t|$ = 0.09 - 0.55 GeV^2

Data sets for combination

- H1 FPS HERA II
  [Eur.Phys.J. C71 (2011) 1578]
  Luminosity = 156.6 pb^{-1}
  Visible range $|t|$ = 0.1 – 0.7 GeV^2
  Norm unc ~ ± 6%

- H1 FPS HERA I
  [Eur.Phys.J. C48 (2006) 749]
  Luminosity = 28.4 pb^{-1}
  Visible range $|t|$ = 0.08 – 0.5 GeV^2
  Norm unc ~ ± 10%

- ZEUS LPS 2
  [Nucl.Phys. B816 (2009) 1]
  Luminosity = 32.6 pb^{-1}
  Visible range $|t|$ = 0.09 – 0.55 GeV^2
  Norm unc ~ +11 -7%

- ZEUS LPS 1
  [Eur.Phys.J. C38 (2004) 43]
  Luminosity = 3.6 pb^{-1}
  Visible range $|t|$ = 0.075 – 0.35 GeV^2
  Norm unc ~ +12% - 10%

$\sigma_r^{D(3)}$ combined

Main H1 and ZEUS detectors used to reconstruct Q^2, W and x, whereas M_x, ß, x_{IP} and t derived from FPS/LPS or from combined info H1+FPS/ZEUS+LPS

Combination performed in the ZEUS visible t range $|t|$ = 0.09 - 0.55 GeV^2

Prior to combining, ZEUS cross section points swam to H1 (Q^2, β, x_{IP}) grid using ZEUS DPDF SJ [Nucl.Phys. B831 (2010) 1]

$\sigma_r^{D(3)}$ for combination

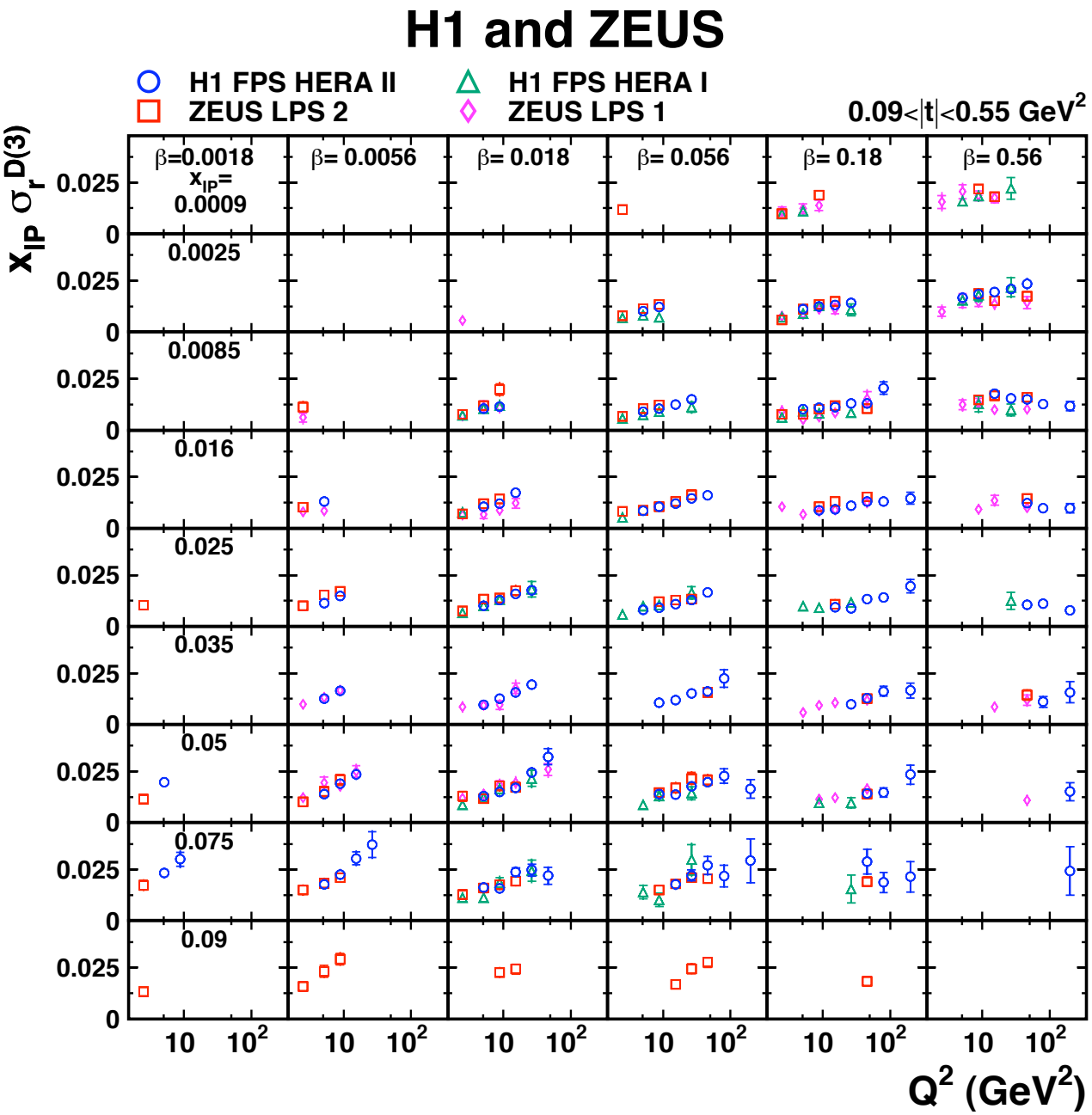

Combination method

- χ^2 minimization which includes full error correlations
[A. Glazov, AIP Conf. Proc. 792 (2005) 237]
- Used for previous combined HERA results [JHEP 1001 (2010) 109]
- Key assumption is that H1 and ZEUS are measuring the same cross sections at the same kinematic points

→ Model independent check of the data consistency and reduction of the systematic uncertainty

Combination method

- χ^2 minimization which includes full error correlations
[A. Glazov, AIP Conf. Proc. 792 (2005) 237]
- Used for previous combined HERA results [JHEP 1001 (2010) 109]
- Key assumption is that H1 and ZEUS are measuring the same cross sections at the same kinematic points

→ Model independent check of the data consistency and reduction of the systematic uncertainty

For a single data set:

$$\chi^2_{\exp}(\vec{m},\vec{b}) = \sum_i \frac{[m^i - \sum_j \gamma^i_j m^i b_j - \mu^i]^2}{\delta^2_{i,stat}\mu^i(m^i - \sum_j \gamma^i_j m^i b_j) + (\delta_{i,uncor} m^i)^2} + \sum_j b_j^2$$

μ^i measured cross section values

m^i combined cross section values

b_j shifts of correlated systematic uncertainty sources in σ units

γ^i_j relative correlated systematic unc.

δ^i_{stat} relative statistical unc.

δ^i_{uncor} relative uncorrelated systematic unc.

Combination method

- χ^2 minimization which includes full error correlations
[A. Glazov, AIP Conf. Proc. 792 (2005) 237]
- Used for previous combined HERA results [JHEP 1001 (2010) 109]
- Key assumption is that H1 and ZEUS are measuring the same cross sections at the same kinematic points

→ Model independent check of the data consistency and reduction of the systematic uncertainty

For a single data set:

$$\chi^2_{\exp}(\vec{m},\vec{b}) = \sum_i \frac{[m^i - \sum_j \gamma^i_j m^i b_j - \mu^i]^2}{\delta^2_{i,stat}\mu^i(m^i - \sum_j \gamma^i_j m^i b_j) + (\delta_{i,uncor} m^i)^2} + \sum_j b_j^2$$

μ^i measured cross section values

m^i combined cross section values

b_j shifts of correlated systematic uncertainty sources in σ units

γ^i_j relative correlated systematic unc.

δ^i_{stat} relative statistical unc.

δ^i_{uncor} relative uncorrelated systematic unc.

Full χ^2_{tot} built from the sum of the χ^2_{exp} of each data set, assuming the individual data sets to be statistically uncorrelated

χ^2_{tot} minimized wrt m^i and b_j

Uncertainties

- Input cross sections published with their statistical and systematic uncertainties; the latter classified into point-to-point uncorrelated and correlated
- Global normalisations included in the fit
- H1 and ZEUS systematic uncertainties treated as independent
- A few procedural uncertainties considered:
  i. additive vs multiplicative nature of the error sources
  ii. correlated systematic error sources ZEUS-H1
  iii. swimming factors applied to ZEUS points
  iv treatment of the uncertainty on the H1 hadronic energy scale
  (in the nominal average taken as correlated separately for $x_{IP} < 0.012$ and $x_{IP} > 0.012$)

Results

352 data points combined to 191 cross section measurements

Good consistency: χ^2/n_{dof} = 133/161

Source	Shift (σ units)	Reduction factor %
FPS HERA II hadronic energy scale $x_{I\!P} < 0.012$	−1.61	56.9
FPS HERA II hadronic energy scale $x_{I\!P} > 0.012$	0.13	99.8
FPS HERA II electromagnetic energy scale	0.49	85.9
FPS HERA II electron angle	0.67	66.6
FPS HERA II β reweighting	0.15	90.4
FPS HERA II $x_{I\!P}$ reweighting	0.05	98.3
FPS HERA II t reweighting	0.70	79.8
FPS HERA II Q^2 reweighting	0.09	97.6
FPS HERA II proton energy	0.05	45.6
FPS HERA II proton p_x	0.62	74.5
FPS HERA II proton p_y	0.27	86.5
FPS HERA II vertex reconstruction	0.07	97.0
FPS HERA II background subtraction	0.84	89.9
FPS HERA II bin centre corrections	−1.05	87.3
FPS HERA II global normalisation	−0.39	84.4
FPS HERA I global normalisation	0.81	48.9
LPS 2 hadronic energy scale	−0.02	55.0
LPS 2 electromagnetic energy scale	−0.14	62.4
LPS 2 $x_{I\!P}$ reweighting	−0.32	98.2
LPS 2 t reweighting	−0.26	86.4
LPS 2 background subtraction	0.40	94.9
LPS 2 global normalisation	−0.53	67.7
LPS 1 global normalisation	0.86	44.1

Table 3: Sources of point-to-point correlated systematic uncertainties considered in the combination. For each source the shifts resulting from the combination in units of the original uncertainty and the values of the final uncertainties as percentages of the original are given.

Results

352 data points combined to 191 cross section measurements

Good consistency: χ^2/n_{dof} = 133/161

Source	Shift (σ units)	Reduction factor %
FPS HERA II hadronic energy scale $x_{I\!P} < 0.012$	−1.61	56.9
FPS HERA II hadronic energy scale $x_{I\!P} > 0.012$	0.13	99.8
FPS HERA II electromagnetic energy scale	0.49	85.9
FPS HERA II electron angle	0.67	66.6
FPS HERA II β reweighting	0.15	90.4
FPS HERA II $x_{I\!P}$ reweighting	0.05	98.3
FPS HERA II t reweighting	0.70	79.8
FPS HERA II Q^2 reweighting	0.09	97.6
FPS HERA II proton energy	0.05	45.6
FPS HERA II proton p_x	0.62	74.5
FPS HERA II proton p_y	0.27	86.5
FPS HERA II vertex reconstruction	0.07	97.0
FPS HERA II background subtraction	0.84	89.9
FPS HERA II bin centre corrections	−1.05	87.3
FPS HERA II global normalisation	−0.39	84.4
FPS HERA I global normalisation	0.81	48.9
LPS 2 hadronic energy scale	−0.02	55.0
LPS 2 electromagnetic energy scale	−0.14	62.4
LPS 2 $x_{I\!P}$ reweighting	−0.32	98.2
LPS 2 t reweighting	−0.26	86.4
LPS 2 background subtraction	0.40	94.9
LPS 2 global normalisation	−0.53	67.7
LPS 1 global normalisation	0.86	44.1

Table 3: Sources of point-to-point correlated systematic uncertainties considered in the combination. For each source the shifts resulting from the combination in units of the original uncertainty and the values of the final uncertainties as percentages of the original are given.

Results

352 data points combined to 191 cross section measurements

Good consistency: χ^2/n_{dof} = 133/161

Source	Shift (σ units)	Reduction factor %
FPS HERA II hadronic energy scale $x_{I\!P} < 0.012$	−1.61	56.9
FPS HERA II hadronic energy scale $x_{I\!P} > 0.012$	0.13	99.8
FPS HERA II electromagnetic energy scale	0.49	85.9
FPS HERA II electron angle	0.67	66.6
FPS HERA II β reweighting	0.15	90.4
FPS HERA II $x_{I\!P}$ reweighting	0.05	98.3
FPS HERA II t reweighting	0.70	79.8
FPS HERA II Q^2 reweighting	0.09	97.6
FPS HERA II proton energy	0.05	45.6
FPS HERA II proton p_x	0.62	74.5
FPS HERA II proton p_y	0.27	86.5
FPS HERA II vertex reconstruction	0.07	97.0
FPS HERA II background subtraction	0.84	89.9
FPS HERA II bin centre corrections	−1.05	87.3
FPS HERA II global normalisation	−0.39	84.4
FPS HERA I global normalisation	0.81	48.9
LPS 2 hadronic energy scale	−0.02	55.0
LPS 2 electromagnetic energy scale	−0.14	62.4
LPS 2 $x_{I\!P}$ reweighting	−0.32	98.2
LPS 2 t reweighting	−0.26	86.4
LPS 2 background subtraction	0.40	94.9
LPS 2 global normalisation	−0.53	67.7
LPS 1 global normalisation	0.86	44.1

Table 3: Sources of point-to-point correlated systematic uncertainties considered in the combination. For each source the shifts resulting from the combination in units of the original uncertainty and the values of the final uncertainties as percentages of the original are given.

Influence of several correlated systematic uncertainties reduced significantly for the combined result

Results

352 data points combined to 191 cross section measurements

Good consistency: χ^2/n_{dof} = 133/161

Source	Shift (σ units)	Reduction factor %
FPS HERA II hadronic energy scale $x_{I\!P} < 0.012$	−1.61	56.9
FPS HERA II hadronic energy scale $x_{I\!P} > 0.012$	0.13	99.8
FPS HERA II electromagnetic energy scale	0.49	85.9
FPS HERA II electron angle	0.67	66.6
FPS HERA II β reweighting	0.15	90.4
FPS HERA II $x_{I\!P}$ reweighting	0.05	98.3
FPS HERA II t reweighting	0.70	79.8
FPS HERA II Q^2 reweighting	0.09	97.6
FPS HERA II proton energy	0.05	45.6
FPS HERA II proton p_x	0.62	74.5
FPS HERA II proton p_y	0.27	86.5
FPS HERA II vertex reconstruction	0.07	97.0
FPS HERA II background subtraction	0.84	89.9
FPS HERA II bin centre corrections	−1.05	87.3
FPS HERA II global normalisation	−0.39	84.4
FPS HERA I global normalisation	0.81	48.9
LPS 2 hadronic energy scale	−0.02	55.0
LPS 2 electromagnetic energy scale	−0.14	62.4
LPS 2 $x_{I\!P}$ reweighting	−0.32	98.2
LPS 2 t reweighting	−0.26	86.4
LPS 2 background subtraction	0.40	94.9
LPS 2 global normalisation	−0.53	67.7
LPS 1 global normalisation	0.86	44.1

Table 3: Sources of point-to-point correlated systematic uncertainties considered in the combination. For each source the shifts resulting from the combination in units of the original uncertainty and the values of the final uncertainties as percentages of the original are given.

Influence of several correlated systematic uncertainties reduced significantly for the combined result

Cross calibration brings average improvement of experimental uncertainty of 27% wrt most precise single data set (FPS HERA II)

Correlated part of experimental uncertainty reduced from about 69% in FPS HERA II to 49%

Results

352 data points combined to 191 cross section measurements

Good consistency: χ^2/n_{dof} = 133/161

Statistical uncertainty: 11%

Statistical + correlated + uncorrelated: 13.8%

Procedural uncertainty: 2.9%

Total uncertainty on cross section 14.3% on average and 6% for most precise points

Normalization uncertainty: 4%

Kinematic coverage extended wrt single input measurements

Q^2 = 2.5 - 200 GeV^2
β = 0.0018 - 0.816
x_{IP} = 0.00035 - 0.09
$|t|$ = 0.09 - 0.55

At low x_{IP}, where the proton spectrometer data are free from proton dissociation background, these combined data provide the most precise determination of the absolute normalisation of the diffractive cross section

Combined $\sigma_r^{D(3)}$

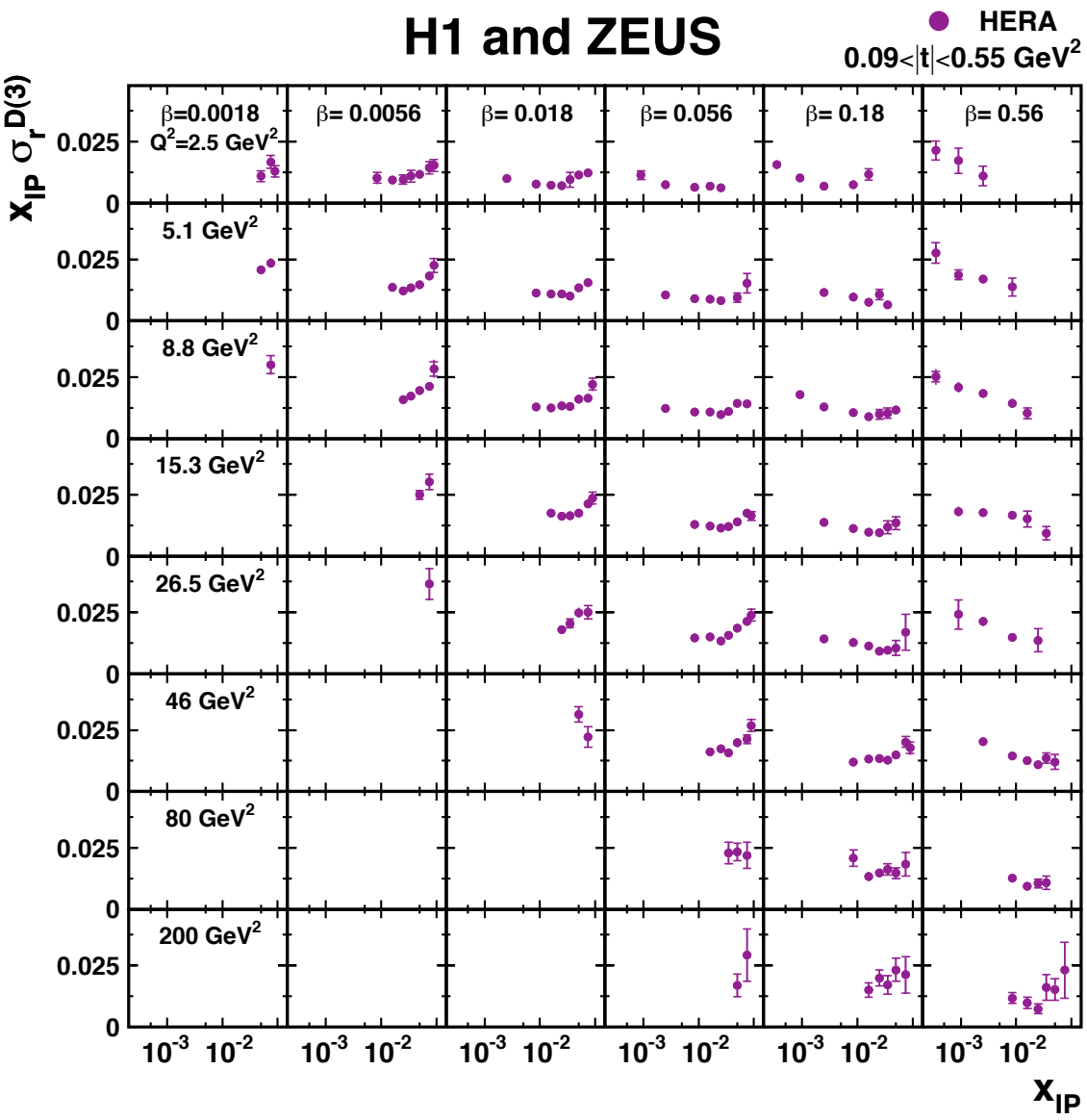

Combined $\sigma_r^{D(3)}$

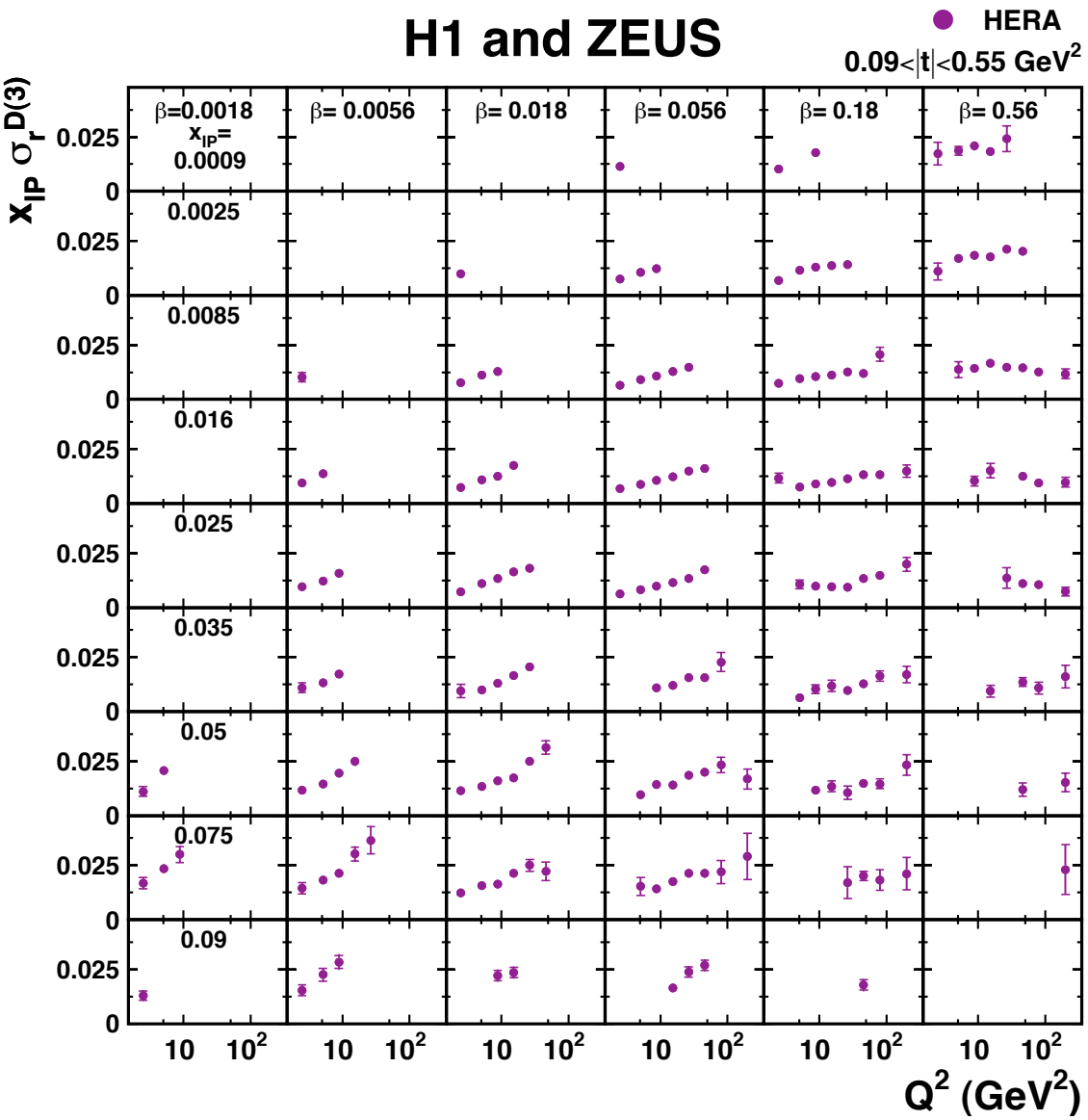

Nice and precise measurement of the scaling violation in diffraction

Combined $\sigma_r^{D(3)}$

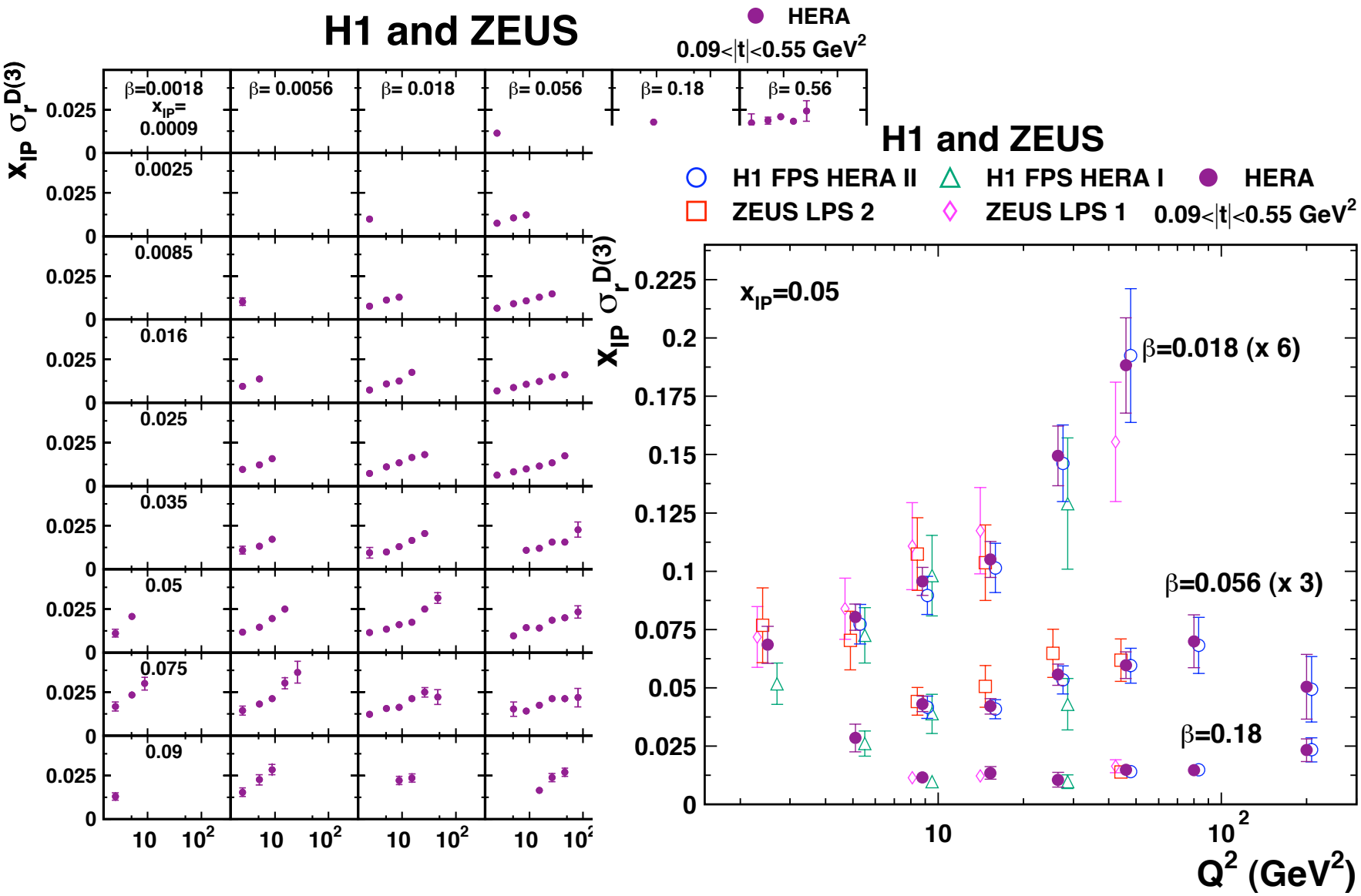

Summary

- In 15 years of running HERA provided unique diffractive data
- First combination of the H1 and ZEUS diffractive data
  - combined proton-tag results
  - consistency between datasets
  - the two experiments calibrate each other resulting in a reduction of the systematic uncertainties
  - most precise determination of the absolute normalisation of the ep → eXp cross section
- Looking forward to combining the LRG data

Backup

$\sigma_r^{D(4)}$ from proton spectrometers

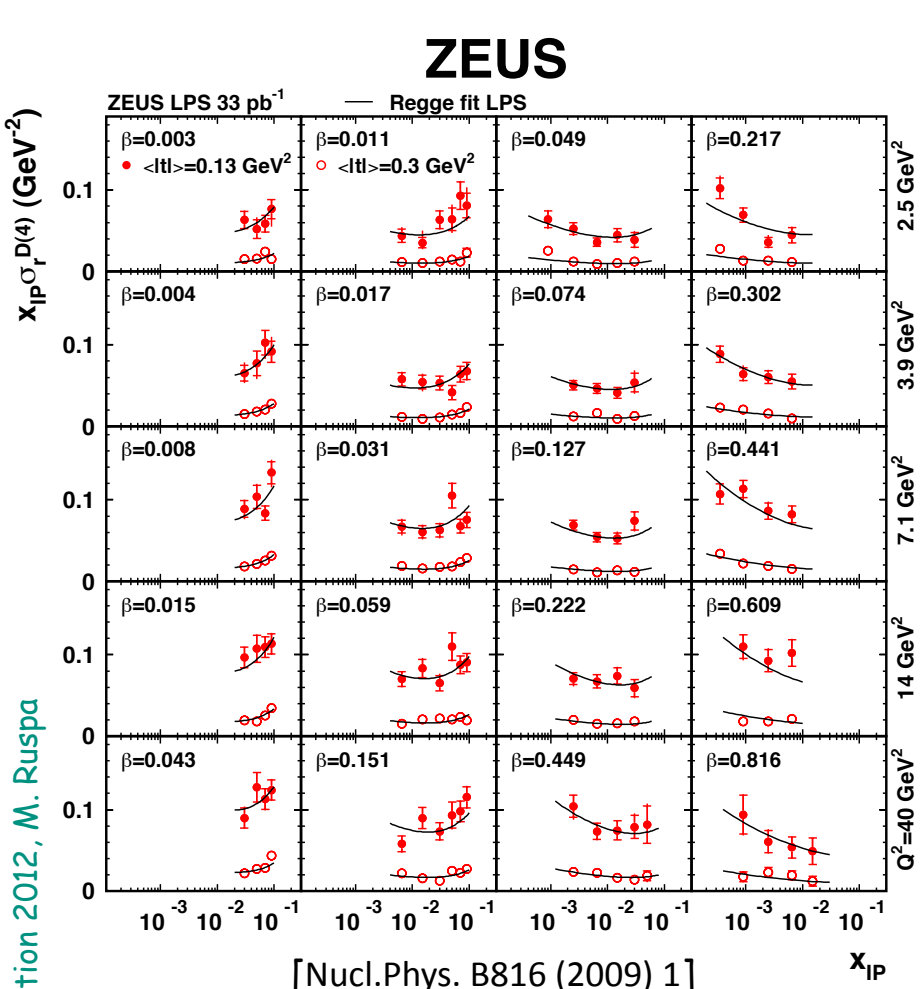

[Nucl.Phys. B816 (2009) 1]

t range 0.09 - 0.55 GeV^2

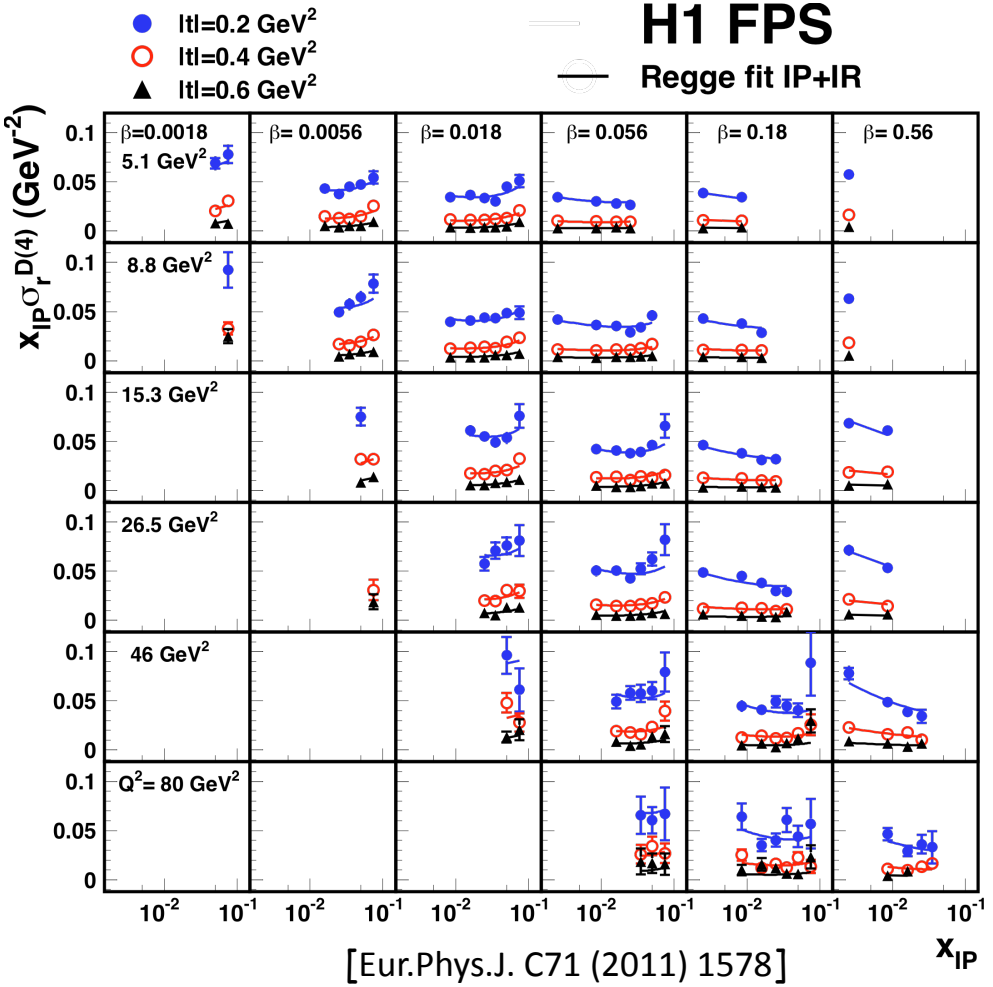

[Eur.Phys.J. C71 (2011) 1578]

t range 0.1 - 0.7 GeV^2

Precise measurement of $\sigma_r^{D(4)}$ in bins of |t|

t-slope

$d\sigma/dt \sim e^{bt}$

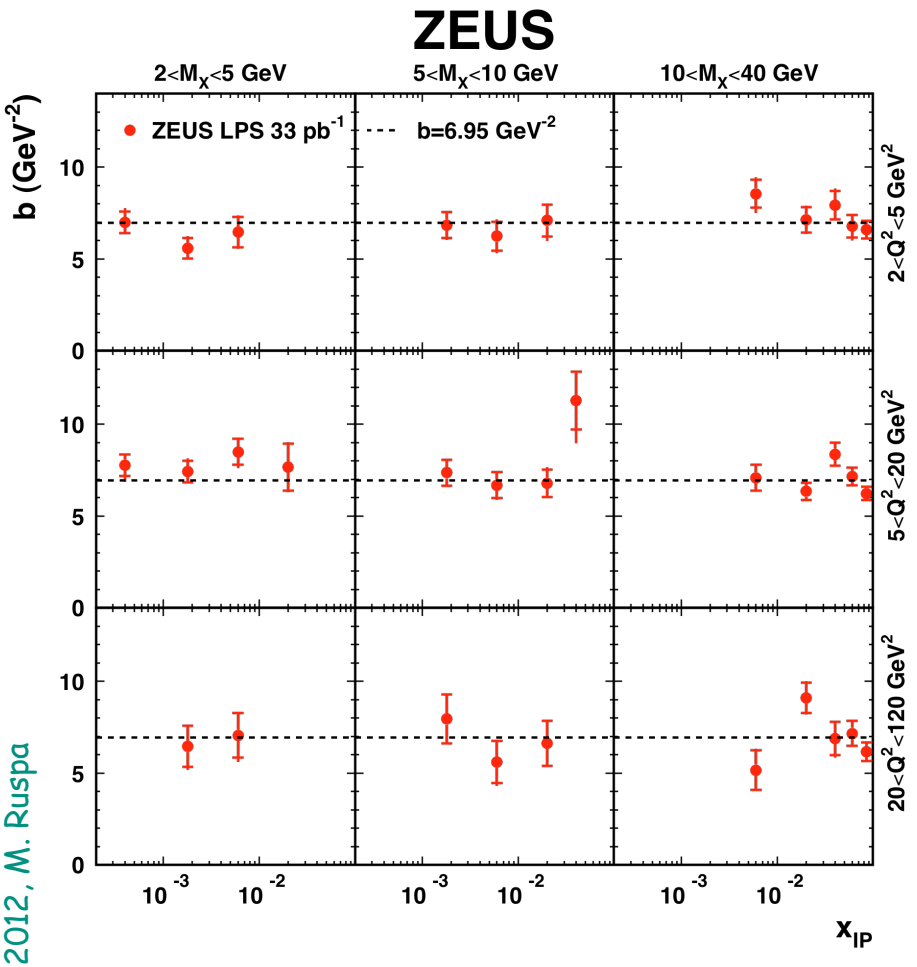

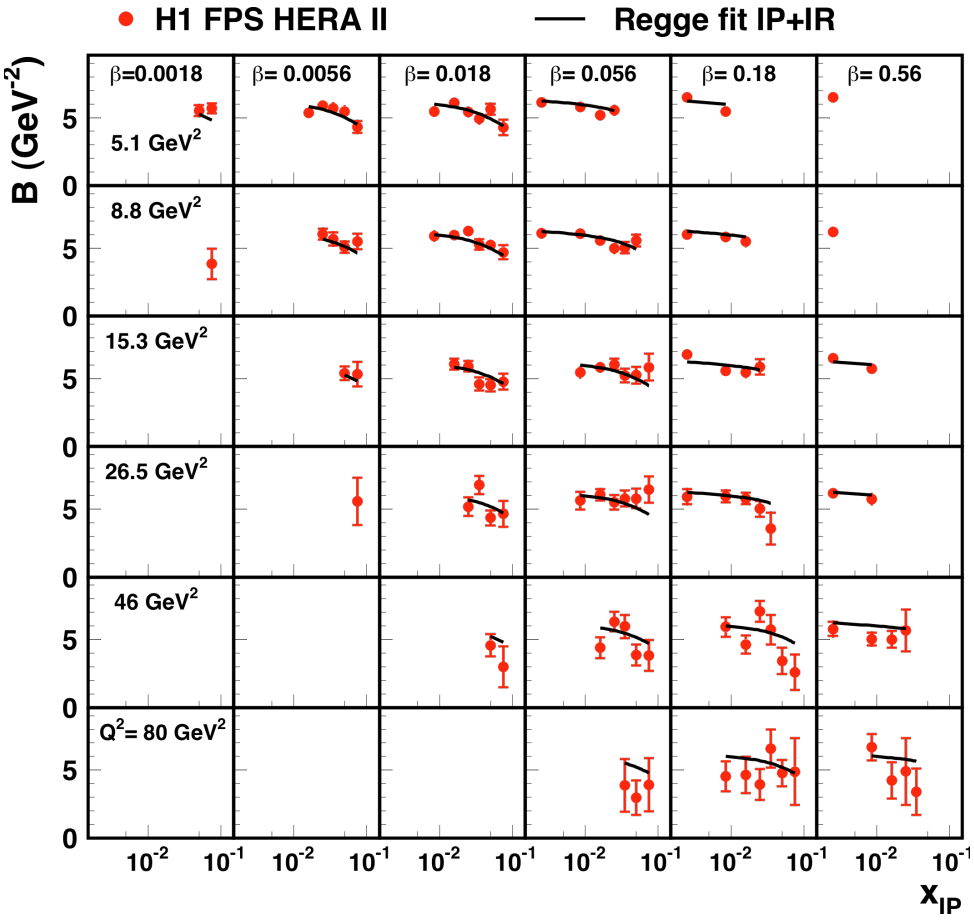

ZEUS t-slope equal to 7 GeV^{-2} (constant through the kinematics)

H1 t-slope between 5 and 6 GeV^{-2} (depending on x_{IP})

$\sigma_r^{D(3)}$ from proton spectrometers

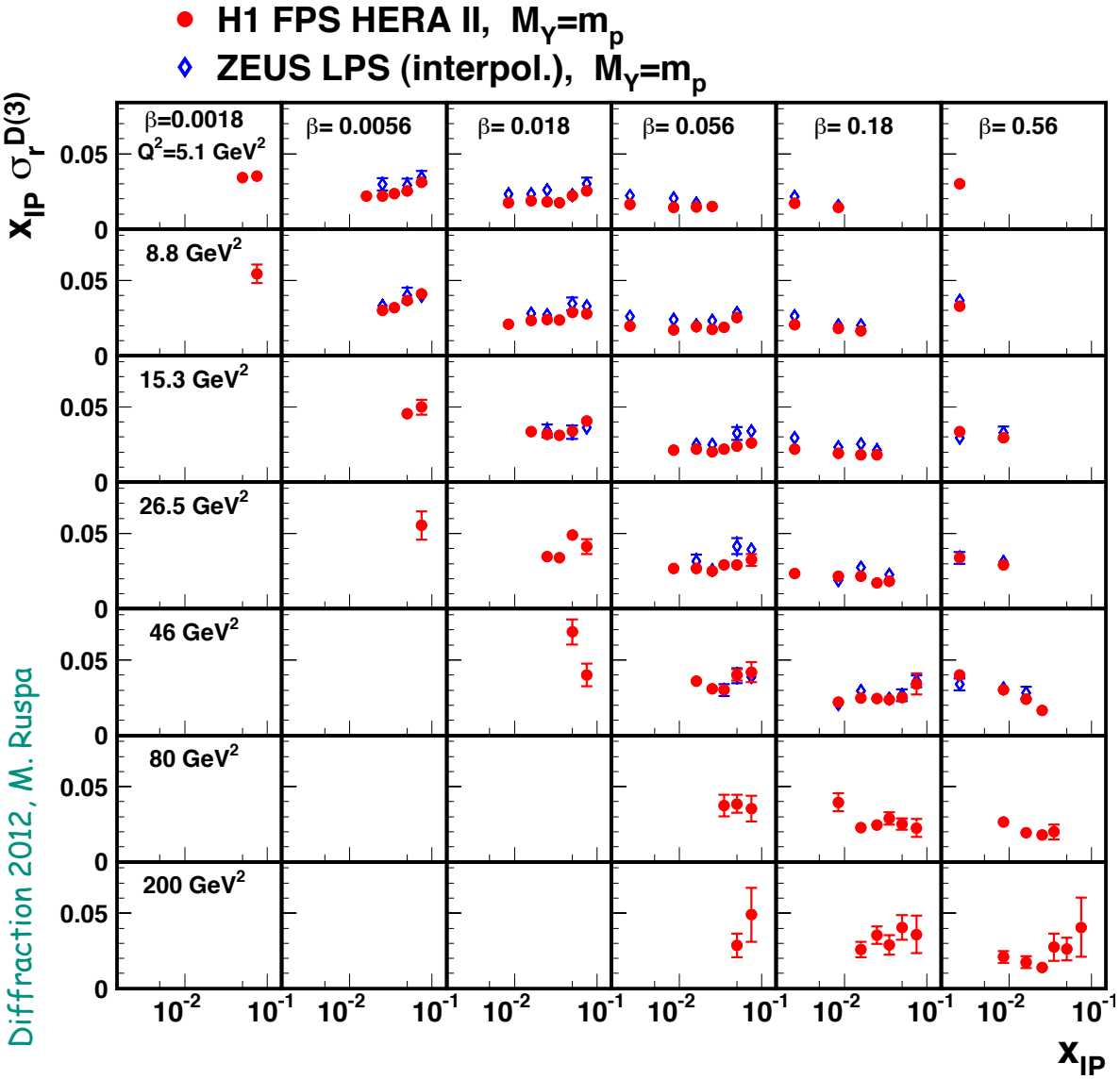

$$\sigma_r^{D(3)} = \int_{-1}^{t_{min}} \sigma_r^{D(4)}\, dt$$

The measured b parameters are used to perform the integration to the range $|t| < 1$ GeV^2

Good agreement in shape between H1 and ZEUS

Fair agreement in normalization between H1 and ZEUS

H1 FPS HERA II norm unc ~ ± 6%
ZEUS LPS norm unc ~ + 11% - 7%

H1 FPS HERA II / ZEUS LPS =
0.85 ± 0.01 (stat) ± 0.03(syst)
+ 0.09 – 0.12 (norm)

Data Set	Q^2 range [GeV^2]	$x_{I\!P}$ range	y range	β range	t range [GeV^2]	Luminosity [pb^{-1}]	Ref.
H1 FPS HERA II	$4-700$	<0.1	$0.03-0.8$	$0.001-1$	$0.1-0.7$	156.6	[2]
H1 FPS HERA I	$2-50$	<0.1	$0.02-0.6$	$0.004-1$	$0.08-0.5$	28.4	[1]
			W range [GeV]	M_X range [GeV]			
ZEUS LPS 2	$2.5-120$	$0.0002-0.1$	$40-240$	$2-40$	$0.09-0.55$	32.6	[4]
ZEUS LPS 1	$2-100$	<0.1	$25-240$	>1.5	$0.075-0.35$	3.6	[3]

Table 1: H1 and ZEUS data sets used for the combination.

Data Set	$\lvert t_{\min}\rvert < \lvert t\rvert < 1$ GeV^2	$0.09 < \lvert t\rvert < 0.55$ GeV^2
FPS HERA II	$\pm 6\%$	$\pm 5\%$
FPS HERA I	$\pm 10\%$	$\pm 10\%$
LPS 2	$+11\%, -7\%$	$\pm 7\%$
LPS 1	$+12\%, -10\%$	$\pm 11\%$

Table 2: Normalisation uncertainties in the full range $|t| < 1$ GeV^2 and in the restricted t range for the data used for the combination.

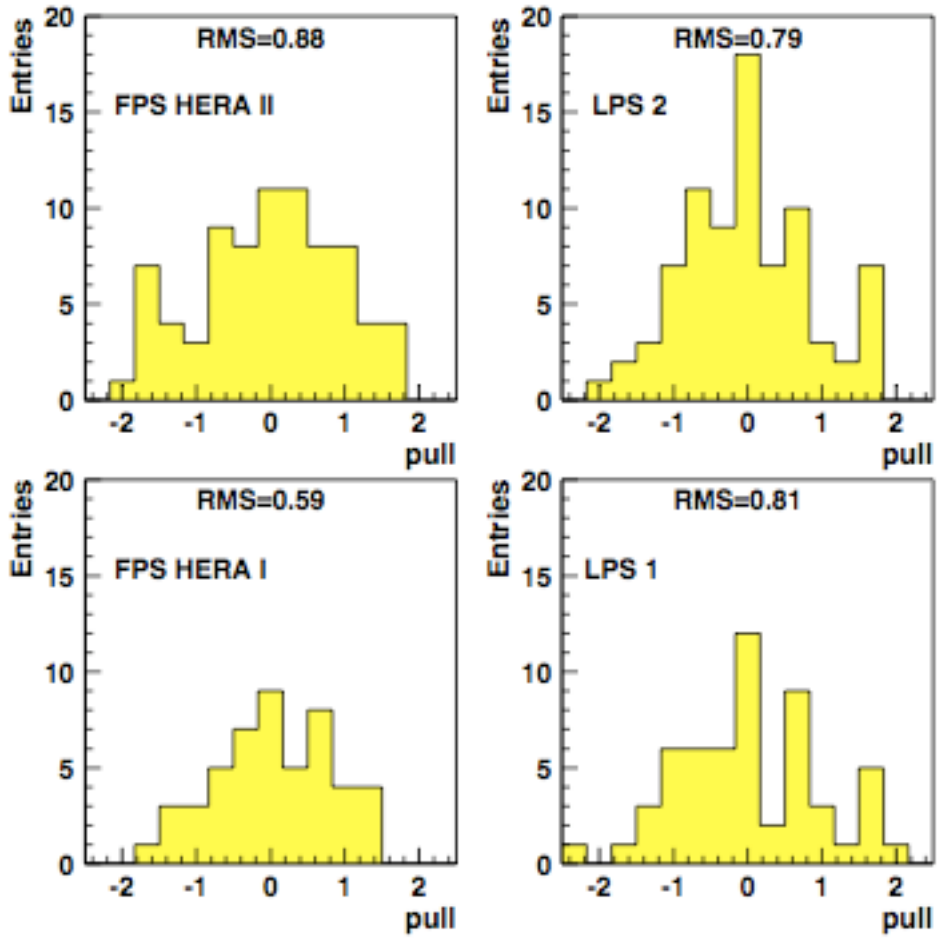

Fig. 3: Pull distributions for the individual data sets. The root mean square gives the root mean square of the distributions.